A comparison of the Gauss-Newton and quasi-Newton methods in resistivity imaging inversion

Loke, MH; Dahlin, Torleif

Published in:
Journal of Applied Geophysics

DOI:
10.1016/S0926-9851(01)00106-9

2002

ELSEVIER

Journal of Applied Geophysics 49 (2002) 149–162

JOURNAL OF APPLIED GEOPHYSICS

www.elsevier.com/locate/jappgeo

A comparison of the Gauss–Newton and quasi-Newton methods in resistivity imaging inversion

M.H. Loke [a,*], T. Dahlin [b,1]

[a] School of Physics, Universiti Sains Malaysia, 11800 USM, Penang, Malaysia
[b] Department of Geotechnology, Lund University, Box 118, S-221 00 Lund, Sweden

Received 18 October 2000; accepted 30 October 2001

Abstract

The smoothness-constrained least-squares method is widely used for two-dimensional (2D) and three-dimensional (3D) inversion of apparent resistivity data sets. The Gauss–Newton method that recalculates the Jacobian matrix of partial derivatives for all iterations is commonly used to solve the least-squares equation. The quasi-Newton method has also been used to reduce the computer time. In this method, the Jacobian matrix for a homogeneous earth model is used for the first iteration, and the Jacobian matrices for subsequent iterations are estimated by an updating technique. Since the Gauss–Newton method uses the exact partial derivatives, it should require fewer iterations to converge. However, for many data sets, the quasi-Newton method can be significantly faster than the Gauss–Newton method. The effectiveness of a third method that is a combination of the Gauss–Newton and quasi-Newton methods is also examined. In this combined inversion method, the partial derivatives are directly recalculated for the first two or three iterations, and then estimated by a quasi-Newton updating technique for the later iterations. The three different inversion methods are tested with a number of synthetic and field data sets. In areas with moderate (less than 10:1) subsurface resistivity contrasts, the inversion models obtained by the three methods are similar. In areas with large resistivity contrasts, the Gauss–Newton method gives significantly more accurate results than the quasi-Newton method. However, even for large resistivity contrasts, the differences in the models obtained by the Gauss–Newton method and the combined inversion method are small. As the combined inversion method is faster than the Gauss–Newton method, it represents a satisfactory compromise between speed and accuracy for many data sets.

Keywords: Quasi-Newton; Gauss–Newton; Optimisation; Resistivity; Imaging; 2D

1. Introduction

One of the recent developments in the resistivity surveying method is the use of two-dimensional (2D) electrical imaging surveys (Griffiths and Barker, 1993). These techniques can be used in areas with moderately complex geology where the conventional resistivity sounding method does not give sufficiently accurate results. A three-dimensional (3D) survey (Loke and Barker, 1996b) should give even more accurate results but at a much greater cost. In many areas, particularly with elongated geological structures, a 2D resistivity survey is probably the most cost-effective method (Dahlin, 1996).

* Corresponding author. Tel.: +60-4-657-7888; fax: +60-4-657-9150.
E-mail addresses: mhloke@pc.jaring.my (M.H. Loke), Torleif.Dahlin@tg.lth.se (T. Dahlin).
[1] Tel.: +46-46-222-9658; fax: +46-46-222-9127.

0926-9851/02/$ - see front matter
PII: S0926-9851(01)00106-9

Many electrical imaging surveys are carried out by small geophysical companies for engineering, environmental and mining studies. In many cases, the survey and data interpretation are carried out by non-geophysicists. As such, a rapid automatic inversion method that can be used on commonly available microcomputers is needed. The Gauss–Newton least-squares method has been used successfully for 2D and 3D inversion of apparent resistivity data (Sasaki, 1989; deGroot-Hedlin and Constable, 1990; Oldenburg and Li, 1994). One possible disadvantage of this technique is the large computing time needed for the calculation of the Jacobian matrix of partial derivatives. Loke and Barker (1996a) used the Jacobian matrix for a homogeneous earth model in the first iteration and a quasi-Newton method to estimate the Jacobian matrix in the later iterations. For some data sets, this method can be several times faster than the Gauss–Newton method. In theory, since the Gauss–Newton method uses the exact Jacobian matrix, it should require fewer iterations to converge than the quasi-Newton method. In this paper, a third method that combines the accuracy of the Gauss–Newton method with speed of the quasi-Newton method is also examined.

The following section briefly describes the Gauss–Newton and quasi-Newton optimisation techniques. It is followed by results from several tests with the Gauss–Newton, quasi-Newton and the proposed combined optimisation method (Loke and Dahlin, 1997).

2. Smoothness-constrained least-squares optimisation method

An example of a 2D inversion model consisting of a number of rectangular cells that is used in this paper is shown in Fig. 1. The arrangement of the cells approximately follows the distribution of the data points in the apparent resistivity pseudosection. The inversion problem is to find the resistivity of the cells that will minimise the difference between the calculated and measured apparent resistivity values. In the smoothness-constrained least-squares method (deGroot-Hedlin and Constable, 1990; Rodi and Mackie, 2001), the following objective function is minimised:

$$\Psi(\mathbf{r}_i) = \mathbf{g}_i^{\mathrm{T}}\mathbf{g}_i + \lambda_i \mathbf{r}_i^{\mathrm{T}}\mathbf{C}^{\mathrm{T}}\mathbf{C}\mathbf{r}_i, \qquad (1)$$

where i is the iteration number, $\mathbf{g}_i$ is the discrepancy vector which contains the differences between the logarithms of the measured and calculated apparent resistivity values, λ_i is the damping factor, $\mathbf{C}$ is a roughness filter matrix and $\boldsymbol{r}_i$ is the model parameters (the logarithm of the model resistivity values) vector.

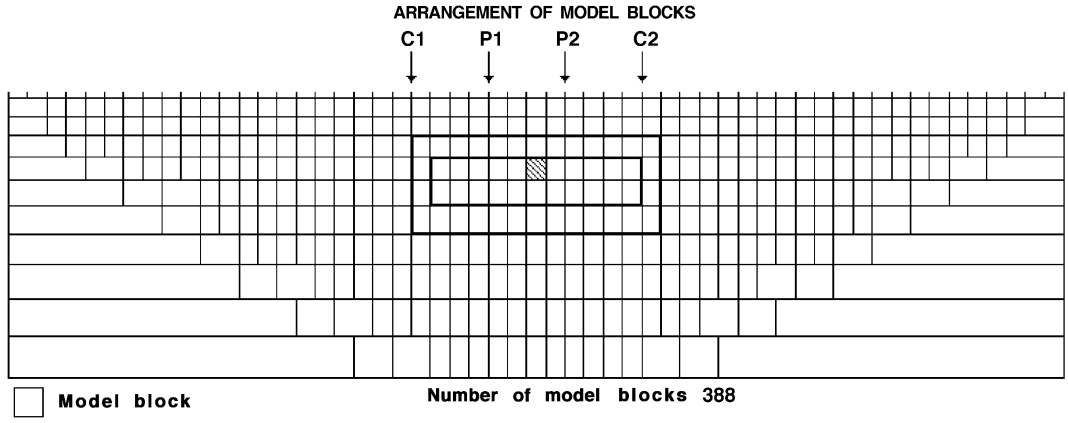

Fig. 1. Subsurface model used by the inversion program for the synthetic test data set. The outline of the rectangular prism model is also shown, as well as the arrangement of the electrodes and shaded model cell for the selected Jacobian matrix value in Fig. 4. The inner prism in the centre of the model has a resistivity of 500 Ω m while the background medium has a resistivity of 10 Ω m. Surrounding the inner prism is a transition zone with a resistivity of 70 Ω m.

The gradient of the objective function (Rodi and Mackie, 2001) is given by:

$$\nabla \Psi(\mathbf{r}_i) = -2\mathbf{J}_i^{\mathrm{T}}\mathbf{g}_i + 2\lambda_i \mathbf{C}^{\mathrm{T}}\mathbf{C}\mathbf{r}_i. \quad (2)$$

The Gauss–Newton method involves the solution of the following system of equations (Sasaki, 1989; Oldenburg and Li, 1994):

$$(\mathbf{J}_i^{\mathrm{T}}\mathbf{J}_i + \lambda_i \mathbf{C}^{\mathrm{T}}\mathbf{C})\mathbf{p}_i = \mathbf{J}_i^{\mathrm{T}}\mathbf{g}_i - \lambda_i \mathbf{C}^{\mathrm{T}}\mathbf{C}\mathbf{r}_{i-1}, \quad (3)$$

where $\mathbf{p}_i$ is the perturbation vector to the model parameters. In the inversion algorithm used in this research, the damping factor parameter is initially set at a large value (λ_0), and it is progressively reduced after each iteration until it reaches the minimum limit (λ_m) selected (Loke and Barker, 1996a). The minimum damping factor λ_m is usually set at one-tenth the value of the initial damping factor λ_0. The value of the initial damping factor λ_0 depends on the level of random noise present in the data (Sasaki et al., 1992). A larger value is used for higher levels of noise. We have found that a value between 0.10 and 0.20 for λ_0 gives satisfactory results for most synthetic and field data sets. The damping factor value is reduced by 2.5 times after each iteration, and it reaches the minimum value after the fourth iteration. After the fourth iteration, the damping factor is kept constant at the minimum value selected.

In the Gauss–Newton least-squares method, the Jacobian matrix is recalculated for all iterations. The finite-difference method (Dey and Morrison, 1979) or finite-element method (Sasaki, 1989; Silvester and Ferrari, 1990) that is used to calculate the apparent resistivity values can also be used to calculate the Jacobian matrix values using the adjoint equation method (McGillivray and Oldenburg, 1990). For data sets with a moderate number (about 100–2000 data points), the calculation of the Jacobian matrix can be the most time-consuming step of the inversion process.

In order to reduce the computing time, Loke and Barker (1996a) used a quasi-Newton method (Broyden, 1965) to estimate the Jacobian matrix values. A homogeneous earth model, for which the Jacobian matrix values can be calculated analytically, is used as the starting model. After each iteration, the Jacobian matrix is estimated by using the following updating equation:

$$\mathbf{B}_{i+1} = \mathbf{B}_i + \mathbf{u}_i \mathbf{p}_i^{\mathrm{T}}, \quad (4)$$

where $\mathbf{u}_i = (\Delta\mathbf{y}_i - \mathbf{B}_i\mathbf{p}_i)/\mathbf{p}_i^{\mathrm{T}}\mathbf{p}_i$, $\Delta\mathbf{y}_i = \mathbf{y}_{i+1} - \mathbf{y}_i$ and $\mathbf{B}_{i+1}$ is the approximate Jacobian matrix for the $(i+1)$th iteration, $\mathbf{y}_i$ is the model response for the ith iteration and $\Delta\mathbf{y}_i$ is the change in the model response for the ith iteration. In theory, the convergence rate of the quasi-Newton method is slower than the Gauss–Newton method (Burden et al., 1981). While the quasi-Newton method might require more iterations to converge compared to the Gauss–Newton method, the time taken per iteration can be much less. For models with small resistivity contrasts (less than 10:1), there were no significant differences in the results obtained by the two methods while the computer time taken by the quasi-Newton method was much lower (Loke and Barker, 1996a).

In this paper, a comparison is made of the results obtained with both methods, as well as for cases with larger resistivity contrasts. Since the partial derivative values for a homogenous earth model are used for the starting Jacobian matrix in the quasi-Newton method, the difference between the estimated Jacobian matrix **B** and the true Jacobian matrix **J** is likely to be larger, as the resistivity contrasts in the subsurface model increase. In the following section, we also compare the accuracy of the models obtained by the quasi-Newton and Gauss–Newton methods for cases with small and large resistivity contrasts.

3. Results

In this section, the results from tests conducted using synthetic data and two field data sets are given. The computations were carried out with a 550-MHz Pentium III-based microcomputer with 256 megabytes RAM.

3.1. Rectangular prism model

The test model (Fig. 2) consists of a rectangular prism with a resistivity of 500 Ω m embedded in a medium with a resistivity of 10 Ω m. A transition

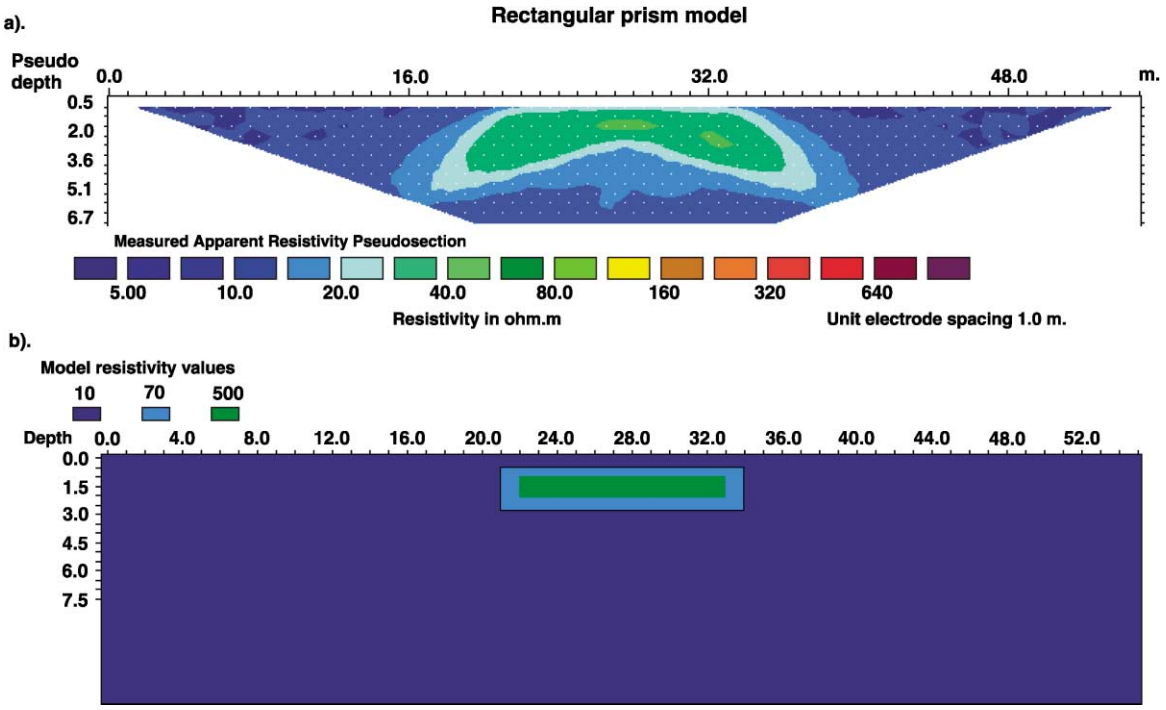

Fig. 2. Test model with apparent resistivity pseudosection. Random noise with amplitude of 2% was added to the apparent resistivity values.

zone of 70 Ω m in between the prism and the background medium is used to simulate a smooth change in the subsurface resistivity. The apparent resistivity values for a multi-electrode system with 56 electrodes using the Wenner array are calculated with a finite-difference program. All the possible 455 apparent resistivity values for electrode spacings of 1–13 m are used as the input data set. Gaussian random noise (Press et al., 1988) of 2% is added to the apparent resistivity values. The resulting apparent resistivity pseudosection is also shown in Fig. 2.

The subsurface model used by the inversion program, which consists of 388 rectangular cells, is shown in Fig. 1. A homogenous earth model with a resistivity of 12.5 Ω m (which is calculated from the average of the logarithms of the apparent resistivity values) is used as the starting model. The starting homogeneous earth model gives an apparent resistivity root mean square (RMS) error of 44%. The RMS error is calculated from the difference between the logarithms of the measured and calculated apparent resistivity values. The change in the RMS error with the computer CPU time (together with the iteration numbers) for the Gauss–Newton inversion method is shown in Fig. 3. The RMS error decreases after each iteration with the largest reductions in the first three

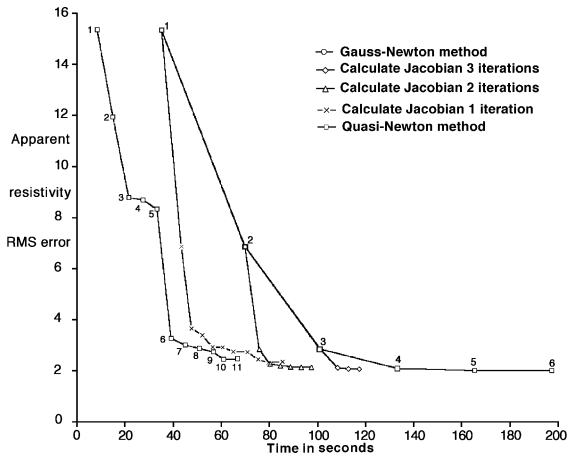

Fig. 3. Change of apparent resistivity RMS error with computer CPU time for the different methods in the inversion of the rectangular prism model data set. The iteration numbers for the Gauss–Newton and quasi-Newton methods are also shown.

iterations. The Gauss–Newton method converges at the fourth iteration with an RMS value of 2.11%, after which there is no significant decrease in the RMS error. Fig. 4a shows the change in the resistivity value of a selected model cell in the middle of the 500-Ω-m prism (shaded in Fig. 1) with iteration number. The change in the Jacobian matrix value for one of the apparent resistivity measurements (the arrangement of the electrodes is shown in Fig. 1) with respect to the cell resistivity is shown in Fig. 4b. The apparent resistivity measurement chosen has a Wenner electrode spacing of 4 m and a median depth of investigation (Edwards, 1977) of about 2 m that lies near the centre of the prism. For the Gauss–Newton method, both the cell resistivity and the Jacobian matrix value show the largest changes in the first two or three iterations. The cell resistivity converges close to the true value of 500 Ω m at the fourth iteration.

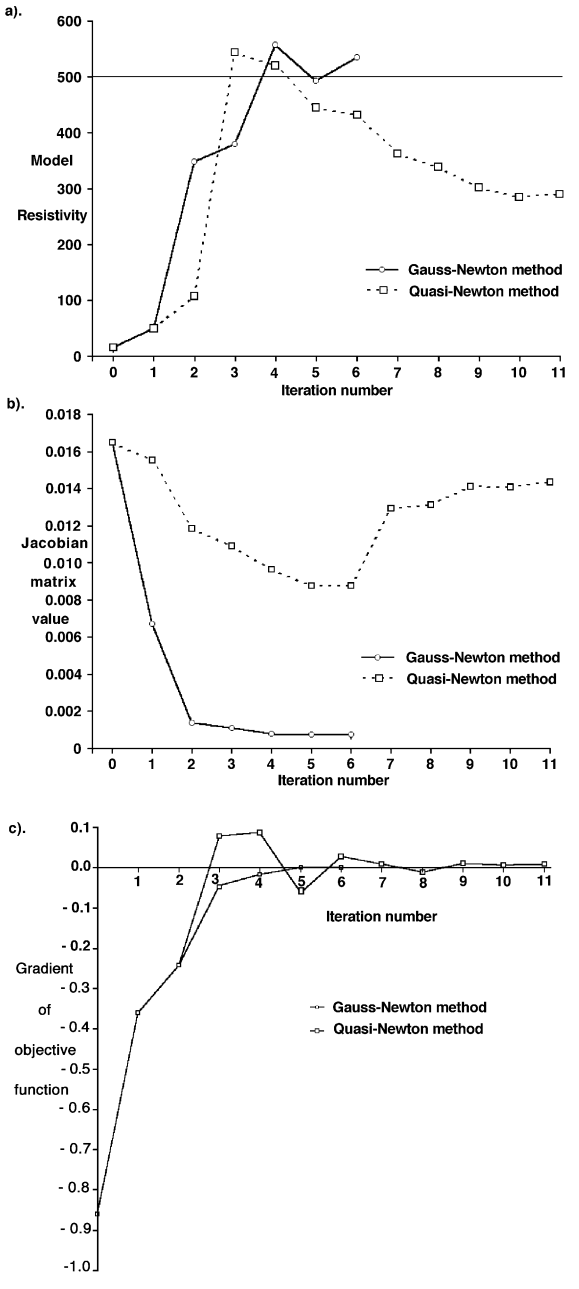

Fig. 4. Change of (a) resistivity value and (b) Jacobian matrix value for the selected array configuration and model cell in Fig. 1, and (c) the gradient of the objective function with respect to the selected model cell.

Fig. 3 also shows the change in the RMS error when the quasi-Newton method is used to estimate the Jacobian matrix. The same set of damping factor values is used for the Gauss–Newton, quasi-Newton, and the combined inversion methods. Note that from the second iteration onwards, the RMS error achieved by the Gauss–Newton method is significantly lower than that obtained with the quasi-Newton method. While the Gauss–Newton method converges in four iterations, the RMS error for the quasi-Newton method is 8.70% at the fourth iteration and slowly decreases to an asymptotic value of about 2.45% after 11 iterations. Further calculations up to 20 iterations did not result in a significantly better inversion model.

Although the RMS error value continues to decrease after the fourth iteration, the model cell resistivity diverges from the true value of 500 Ω m. The poorer result obtained with the quasi-Newton method is probably caused by the method used to estimate the Jacobian matrix. The updating method assumes that the change in the Jacobian matrix values between consecutive iterations is rank-one matrix (Broyden, 1965). However, the actual change can be much more complex. A plot of the Jacobian matrix value (for the selected measurement and model cell shown in Fig. 1) estimated by the quasi-Newton method shows that it decreases in the first six iterations in a similar manner to the Gauss–Newton method, but it does not reach the asymptotic value of about 0.001 achieved by the Gauss–Newton method (Fig. 4b). After the sixth iteration, it increases and diverges from the value given by the Gauss–Newton method.

Fig. 4c shows the gradient of the objective function (Eq. (2)) for the model cell shown in Fig. 1. For the Gauss–Newton method, the gradient value is almost zero after four iterations as it approaches a minimum point of the objective function. However, for the quasi-Newton method, the gradient value oscillates about the zero value and approaches the zero value slowly. Thus, even if the quasi-Newton method eventually converges to the same model as the Gauss–Newton method, the convergence rate might be very slow.

Fig. 3 also shows the change in the RMS error for a combined Gauss–Newton and quasi-Newton method where the Jacobian matrix is recalculated by the finite-difference subroutine for the first iteration only. For the second iteration onwards, the quasi-Newton method is used to estimate the Jacobian matrix. The RMS error curve for this combined method lies in between the error curves for the Gauss–Newton and quasi-Newton methods. It converges more rapidly than the quasi-Newton method from the second iteration onwards, but the convergence rate (in terms of the change in the RMS error per iteration) is still significantly slower than the Gauss–Newton method. When the Jacobian matrix for the combined method is directly recalculated for the first two iterations, its performance is only slightly poorer than the Gauss–Newton method. At the fourth iteration, it gives an RMS value of 2.28% compared to 2.11% for the Gauss–Newton method.

When the Jacobian matrix is recalculated for the first three iterations, there are no significant differences in the results obtained compared with the Gauss–Newton method. This is probably because after the first two or three iterations, the change in the Jacobian matrix values is much smaller than the change in the first two iterations. Thus, the error in the Jacobian matrix values estimated by the quasi-Newton updating method in the later iterations has a smaller effect on the results. In this case, recalculating the Jacobian matrix for the first two or three iterations only can be a good compromise between reducing the computing time while at the same time ensuring that the results are sufficiently accurate.

The quasi-Newton method took 61 s to reduce the RMS error to 2.43%. In comparison, the Gauss–Newton method took 133 s to reduce the RMS error below this value (2.11% after four iterations). The combined inversion methods with one, two and three recalculations took 79 s (2.33% after 10 iterations), 80 s (2.28% after four iterations) and 108 s (2.11% after four iterations).

Besides comparing the time taken by the different inversion methods, it is also important to consider the accuracy of the models obtained. To achieve this, we select the models produced by each method at the iteration, after which no significant improvements were obtained. Fig. 5 shows the inversion models produced by the different inversion methods. The figure also shows the RMS difference between the resistivity values of the model cells compared to the true resistivity values in the synthetic model (Fig. 2). The Gauss–Newton method and the combined methods with two and three recalculations accurately reproduce the high resistivity rectangular prism. The RMS model differences for the models are very similar at about 55.4–56.7%. The variation in the RMS model differences is less than the 2% noise added to the data. While the model produced by the quasi-Newton method after 10 iterations has an RMS error of 2.45%, the high resistivity region has been split into two zones with slightly lower values near the middle of the prism. The RMS model difference is significantly higher at 67.7%. The combined method with one recalculation shows a similar distortion but to a lesser extent. It also has a lower RMS model difference of 60.8%.

3.2. Landfill survey, Germany

This survey was conducted over a landfill site to map the leakage of soluble pollutants from the landfill (Niederleithinger, 1994). It is chosen as an example of a field data set with low resistivity contrasts. The survey was carried out using the Wenner array and the measured apparent resistivity pseudosection is shown in Fig. 6a. Fig. 7 shows the RMS error curves when the different inversion methods are used. The quasi-Newton method converged in four iterations, after which there are only marginal changes in the RMS error. It took 12 s to reduce the RMS error to 1.72%. The combined method with one recalculation took three iterations and 23 s to reduce the RMS error to 1.69%. The Gauss–Newton method took three iterations and 49 s to reduce the RMS error to 1.65%. The results obtained with the combined methods where the Jacobian matrix was recalculated for the first two or three iterations are not shown, as they are almost identical with the

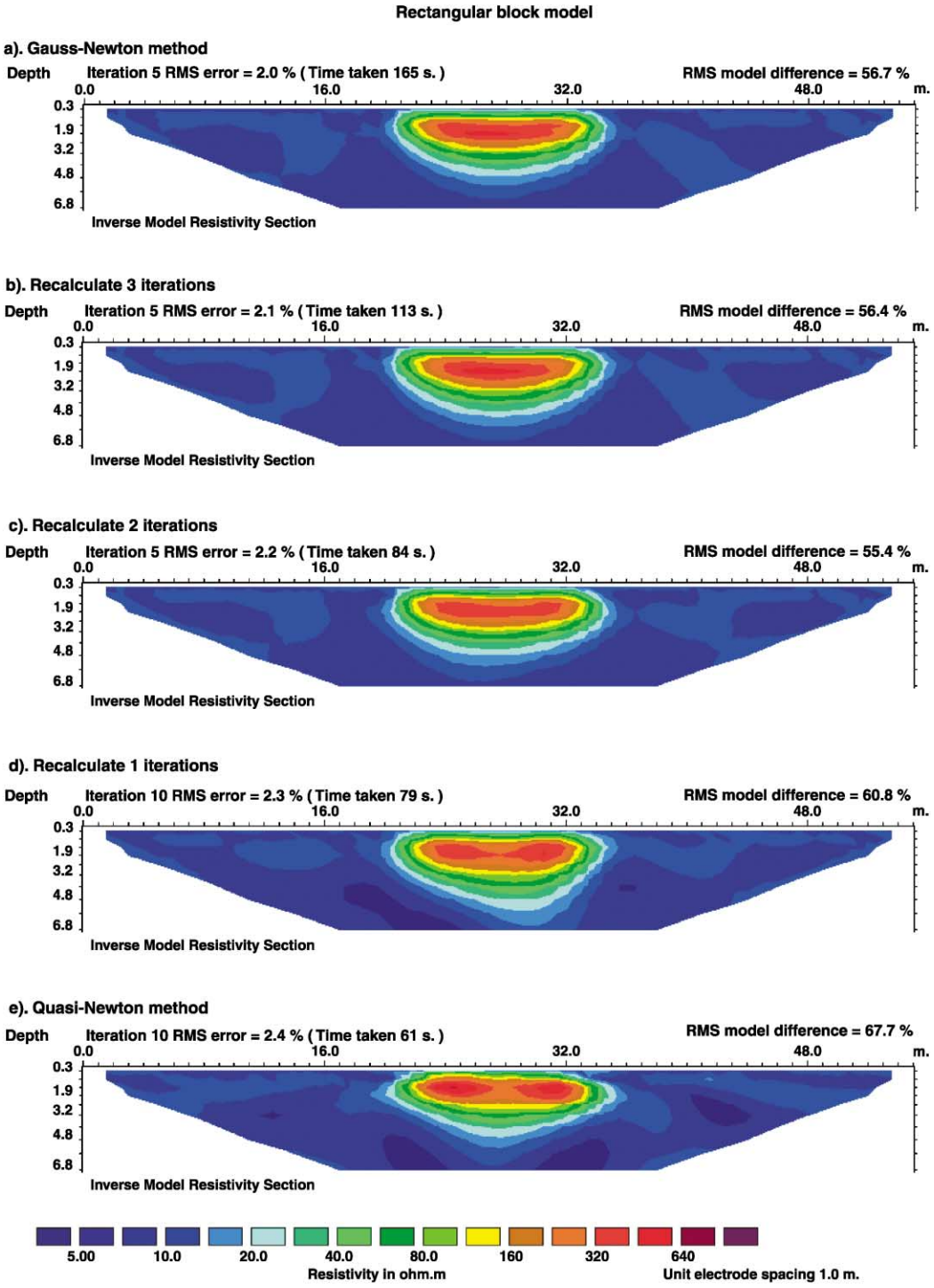

Fig. 5. Inversion models obtained by the (a) Gauss–Newton method, combined methods with (b) three recalculations, (c) two recalculations and (d) one recalculation of the Jacobian matrix, and (e) quasi-Newton method for the synthetic data set.

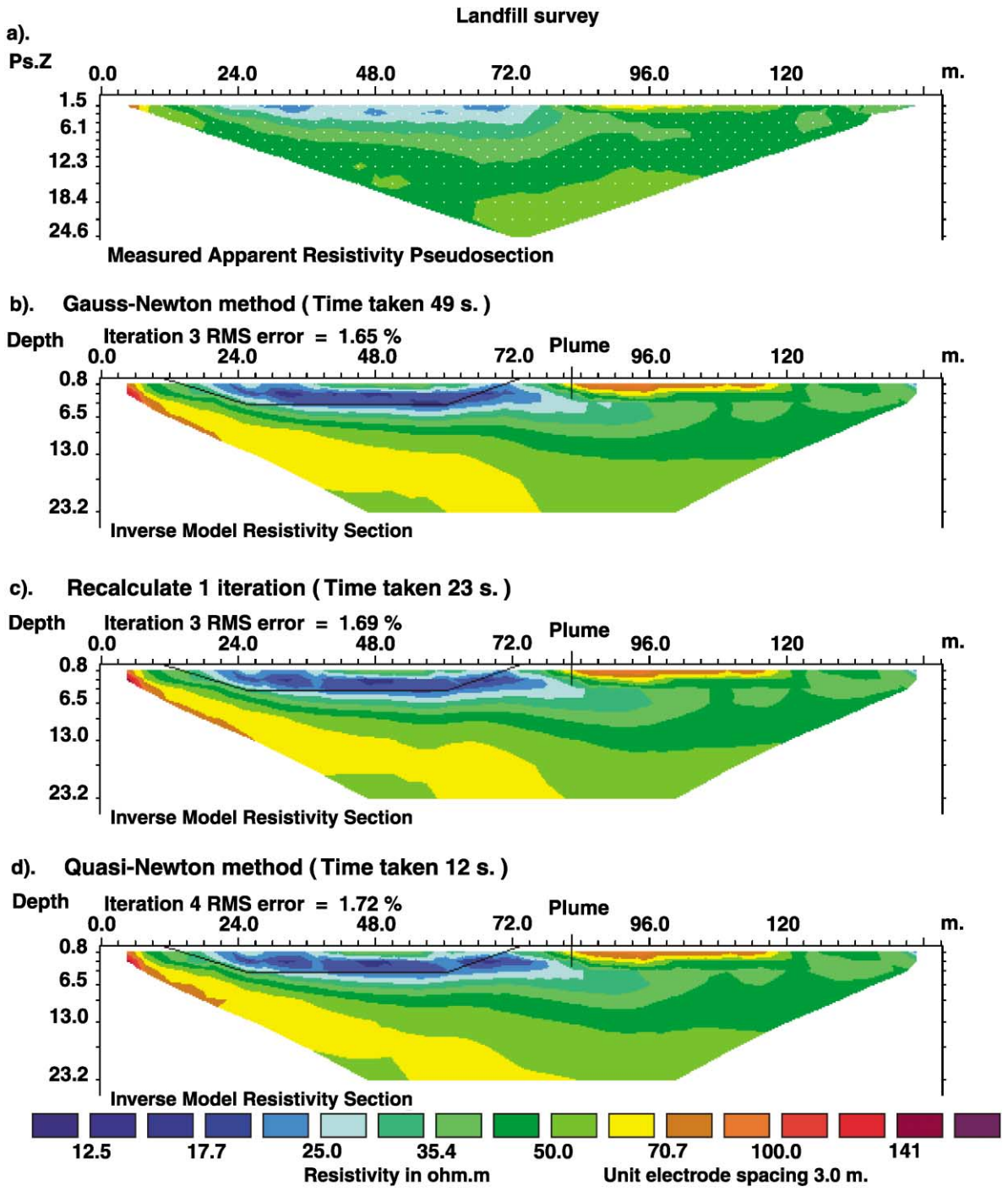

Fig. 6. (a) Apparent resistivity pseudosection from the landfill survey. Inversion models obtained with the (b) Gauss–Newton method, (c) recalculation of the Jacobian matrix for one iteration and (d) quasi-Newton method. The outline of the landfill is superimposed on the inversion models.

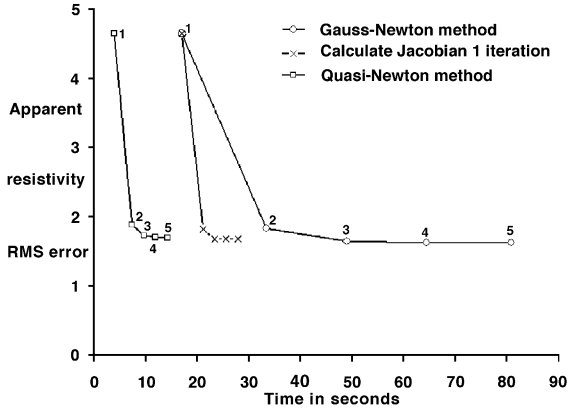

Fig. 7. Change of apparent resistivity RMS error with computer CPU time for the different inversion methods in the inversion of the landfill survey data set. The iteration numbers for the Gauss–Newton and quasi-Newton methods are also shown.

Gauss–Newton method. The inversion models in Fig. 6 do not show any significant differences. All of them show a low resistivity area that agrees with the known boundaries of the landfill, as well as a pollution plume that has leaked through the right boundary of the landfill. The resistivity values in the inversion models show a relatively small range of about 20–200 Ω m. Due to the small resistivity contrasts, the Jacobian matrix for a homogeneous earth model used by the quasi-Newton method is probably a good approximation of the true Jacobian matrix.

3.3. Rock quality survey, Sweden

A number of electrical imaging surveys were carried out in the Hallandsås area in southwest Sweden to access the rock quality along the proposed Hallandsås Railway Tunnel Project (Dahlin et al., 1996, 1999a,b; Dahlin and Sturk, 1998) that involves the construction of two parallel tunnels. The Hallandsås Horst is one of several uplifted blocks in the Scania (Skåne) province in southern Sweden. The horst is composed of Precambrian rocks (consisting of gneiss, amphibolite and dolerite) and is flanked by younger Triassic/Jurassic sedimentary rocks. The horst area is approximately 8–10 km wide, 30–40 km long and has a northwest to southeast trend. The main objective of the surveys was to map zones of fractured and weathered rock along the proposed route that is likely to cause problems during the tunnel's construction. In particular, the softer sedimentary rocks and highly fractured and weathered metamorphic/igneous rocks may create problems if they are not accounted for in the tunnel construction plans. Geological information from two boreholes, KB 9501 and KB 9502, located along the survey line is available to verify the results from the inversion models (Dahlin et al., 1999a). The boreholes were sited on the basis of the electrical imaging survey results, and they revealed the presence of heavily weathered crystalline rocks and sedimentary rocks. Information is also available from measurements of engineering rock properties during the construction of the tunnels. The measurements include the RQD (rock quality designation), Q (tunneling quality index) and weathering grade values (Barton et al., 1974; Goodman, 1993; Dahlin and Sturk, 1998).

Fig. 8a shows the apparent resistivity pseudosection from the survey in the Southern Marginal Zone area (Dahlin et al., 1999a). The inversion model used consists of 2742 cells while the pseudosection has 1743 data points. There is significant topography along the survey line. The topography was incorporated into the inversion model using a distorted finite-element grid such that the surface of the grid matches the actual topography (Tong and Yang, 1990; Silvester and Ferrari, 1990; Sasaki et al., 1992). The distribution of the model cells were initially made using the same method as for a model without topography. The vertical locations of the subsurface model cells were then adjusted using the inverse Schwartz–Christoffel transformation method (Spiegel et al., 1980; Loke, 2000). This results in a distorted finite-element grid where the distortion gradually decreases with depth.

The error curves for the different inversion methods are shown in Fig. 9. The Gauss–Newton method converges after four iterations with an RMS error of 4.3%. The resulting model (Fig. 8b) shows a very large range of resistivity values that ranges from about 30 to 27,000 Ω m. The quasi-Newton method converges to a significantly higher RMS error compared to the Gauss–Newton method. The error curve for the quasi-Newton method drops rapidly in the first four iterations followed by a slower decline to an asymptotic value of about 6.4%. The significantly higher asymptotic RMS value for the quasi-Newton method could be caused by a very poor approximation of the Jacobian matrix (due to the very large resistivity contrast of almost 1000:1) such that the search direc-

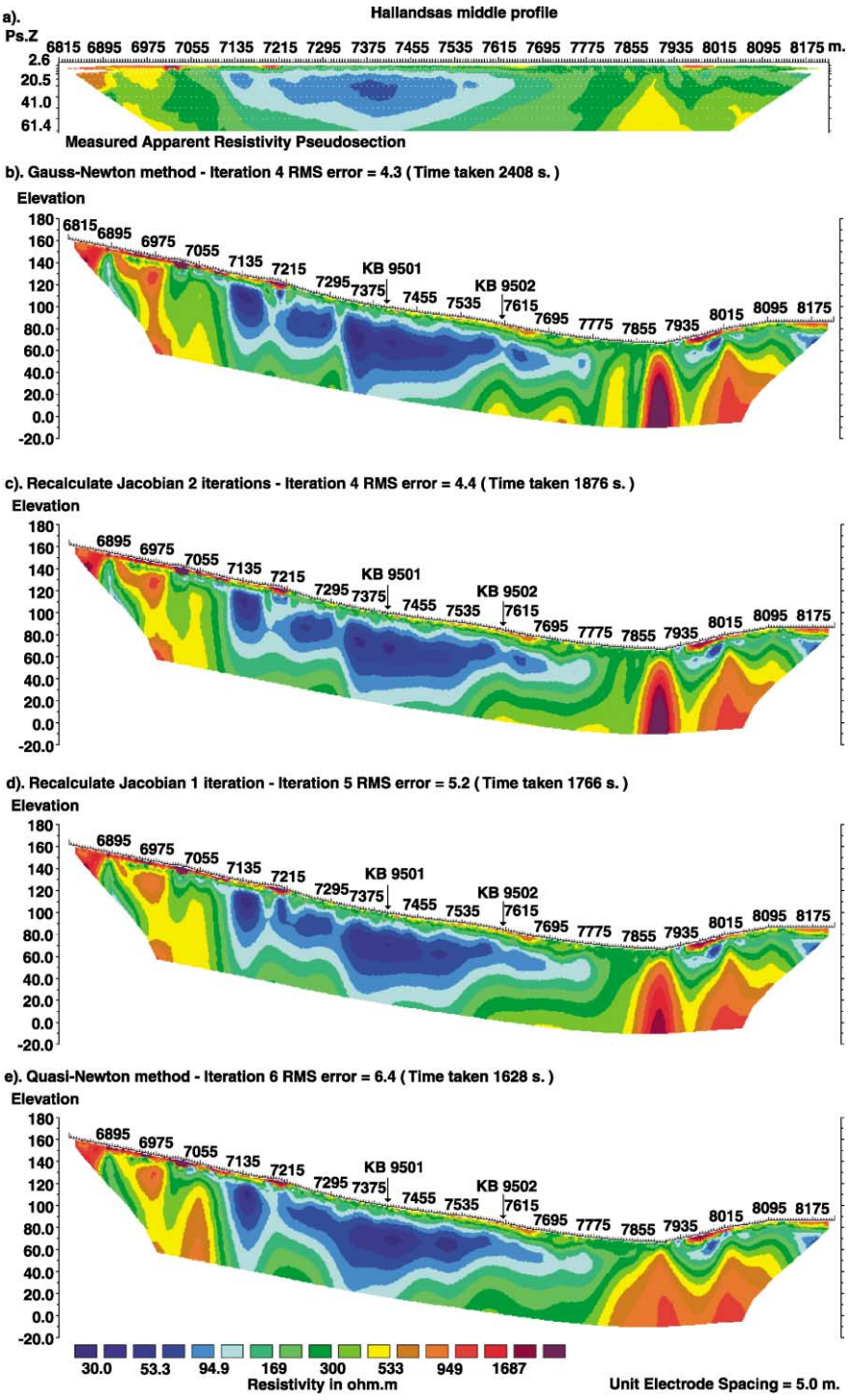

Fig. 8. (a) Apparent resistivity pseudosection from the Hallandsås survey. Inversion models obtained with the (b) Gauss–Newton method, (c) recalculation of the Jacobian matrix for two iterations, (d) recalculation of the Jacobian matrix for one iteration and (e) quasi-Newton method. The locations of two boreholes, KB 9501 and KB 9502, are also shown. The plots of the model sections have a vertical exaggeration factor of 2.

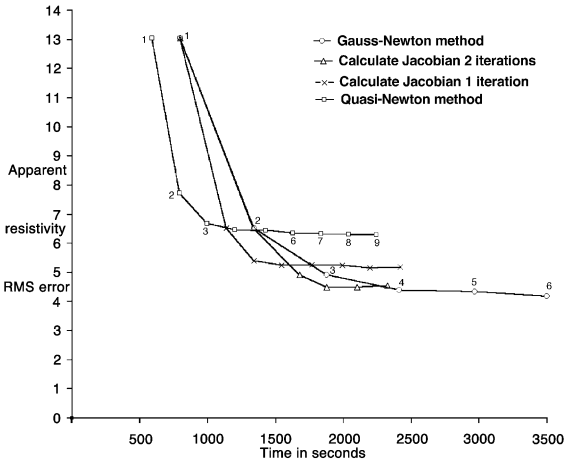

Fig. 9. Change of apparent resistivity RMS error with computer CPU time for the different inversion methods in the inversion of the Hallandsås survey data set. The iteration numbers for the Gauss–Newton and quasi-Newton methods are also shown.

tions used are no longer descent directions (Oldenburg, personal communication) in the later iterations. Another possible reason is that the objective function being minimised in Eq. (1) is not strongly convex and that the quasi-Newton method has converged to a local minimum (Daniels, 1978) that is higher than the minimum reached by the Gauss–Newton method. The quasi-Newton method took six iterations and 1628 s to reduce the RMS error to 6.4%. In comparison, the Gauss–Newton method took 1875 s and three iterations to reduce the RMS error below this value. The combined inversion methods with one and two recalculations took 1340 and 1676 s, respectively, to reduce the RMS error below the asymptotic value achieved by the quasi-Newton method.

Fig. 8 shows the model's sections achieved by the different inversion methods. For each method, we have chosen the result for the last iteration, after which there was no significant reduction in the RMS error. The asymptotic RMS error (4.4%) achieved by the combined method with two recalculations of the Jacobian matrix is very close to the value for the Gauss–Newton method (4.3%). In comparison, the corresponding RMS error with one recalculation of the Jacobian matrix is significantly higher at 5.2%, but less than the value of 6.4% obtained by the quasi-Newton method.

The main structure in the inversion model obtained by the Gauss–Newton method (Fig. 8b) is a low resistivity zone with resistivity values of less than 100 Ω m consisting of the sedimentary and highly weathered metamorphic rocks with a width of about 700 m. The low resistivity zone reaches its thickest extent below the 7350-m mark, which is about 50 m away from the KB 9501 borehole. The low resistivity zone is significantly thinner below the KB 9502 borehole. Fig. 10 shows the model region near the boreholes in greater detail together with the borehole log. There is a good correlation between the model resistivity values and the lithology at both boreholes. At borehole KB 9501, the lowest resistivity values correspond to the sedimentary rocks. Resistivity logging along this borehole gives values of 8–68 Ω m for the sedimentary rocks. Below an elevation level of 60 m, there is a gradual increase in the model resistivity with depth that corresponds to the weathered Precambrian metamorphic and igneous rocks. At borehole KB 9502, the base of the sedimentary rocks was at 50 m elevation followed by a transition layer ranging from highly weathered to weathered and finally to fresh metamorphic/igneous rocks at 22 m elevation near the bottom of the borehole. Again, there is a good correlation between the resistivity model and the lithology. The lowest resistivity values correspond to the sedimentary rocks. This is followed by a relatively rapid increase in the resistivity values, compared to borehole KB 9501, due to a thinner transitional layer of weathered metamorphic/igneous rocks.

Fig. 11 shows a plot of the model resistivity values obtained with the Gauss–Newton method together with the RQD, *Q* and weathering grade values measured in the SE and SW tunnels. One significant feature is the large variation of the RQD, *Q* and weathering grade values between the measurements in the two tunnels. This is probably because the engineering measurements are essentially "point" measurements that depend mainly on the rock properties within a few metres of the sampling point. In comparison, the resistivity values give the average value for a much larger volume (probably in the order of tens of metres) of the subsurface. Despite the scatter in the engineering measurement values, there is a good correlation between the low resistivities between the 7350- and 7550-m marks and the high RQD, *Q* and weathering grade values. In this section, the main rock type within the tunnels is highly weathered amphibolite and gneiss with some sedi-

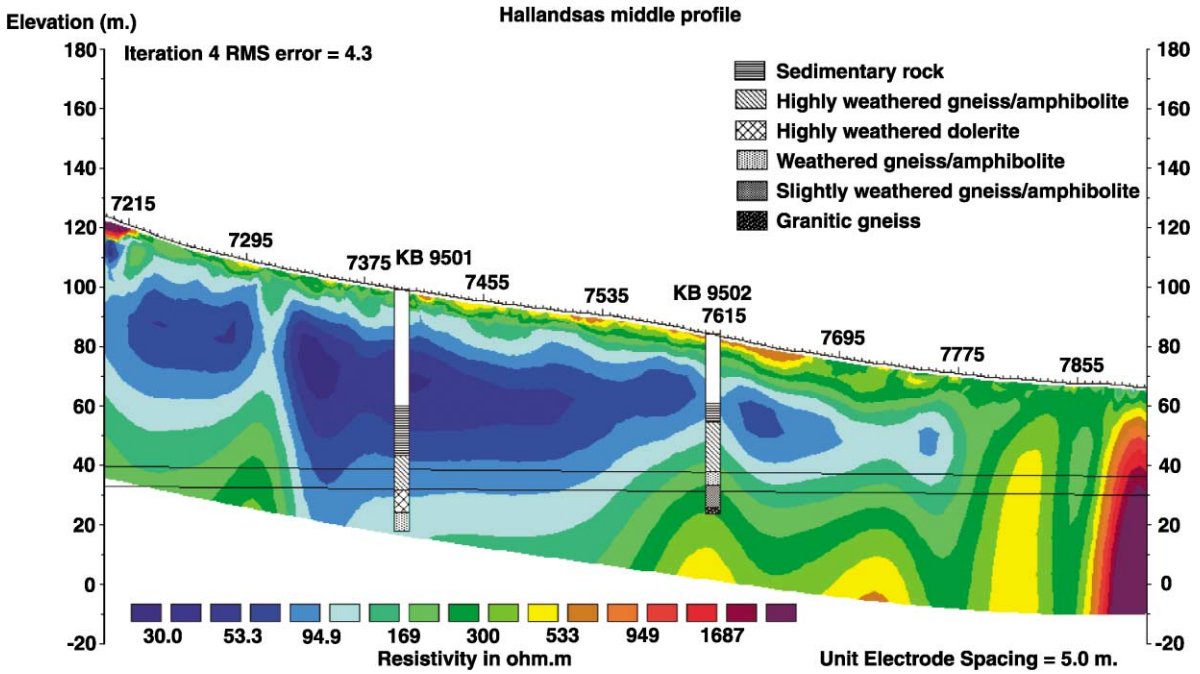

Fig. 10. The central section of the Hallandsås survey model obtained with the Gauss–Newton method with the lithology log for the KB 9501 and KB9502 boreholes. The proposed tunnel route is shown by the pair of lines between elevation levels of about 20–40 m.

mentary rocks in the SE tunnel. In the remaining section of the profile from the 7550- to 8000-m marks, the rocks in the tunnel are amphibolite and gneiss with different degrees of weathering. There is a narrower zone with high RQD, Q and weathering grade values near the 7950-m mark that also corresponds to a low resistivity zone. In the resistivity model section (Fig. 8b), there is a relatively narrow and thin low resistivity zone in this area above the tunnels. Thus, there is generally good agreement between the Gauss–Newton model and the available borehole and tunnel information.

The main features in the inversion models obtained by the quasi-Newton method (Fig. 8e) and the combined methods (Fig. 8c and d) are generally similar to that obtained by the Gauss–Newton method. All the models show the thick sedimentary layer at borehole KB 9501 and a thinner layer at KB 9502, although the boundaries are less sharp compared to the Gauss–Newton model. The main differences, particularly for the quasi-Newton method and the combined method with one recalculation (Fig. 8d and c), are in the secondary structures that are less well resolved.

In the Gauss–Newton model, there is a prominently very high resistivity (of over 1000 Ω m) vertical dyke-like structure below the 7900-m mark with another high resistivity (of about 500 Ω m) vertical structure below 7830-m mark (Fig. 8b). The model obtained with two recalculations of the Jacobian matrix also shows the very high resistivity structure below the 7900-m mark but the second high resistivity vertical structure below the 7830-m mark is less prominent. The quasi-Newton method (Fig. 8e) and the combined method with one recalculation (Fig. 8d) have significantly poorer model resolution, particularly between the 7800- and 7900-m marks, where it is not able to resolve the second high resistivity structure below the 7830-m mark. The very high resistivity structure below the 7900-m mark is significantly sharper with one recalculation (Fig. 8d) but the second high resistivity structure is still not resolved.

However, it should be noted that quasi-Newton method correctly resolves the main features of the section, such as the broad low resistivity sedimentary layer and the thinning of the low resistivity layer at borehole KB 9502. The model given by the quasi-

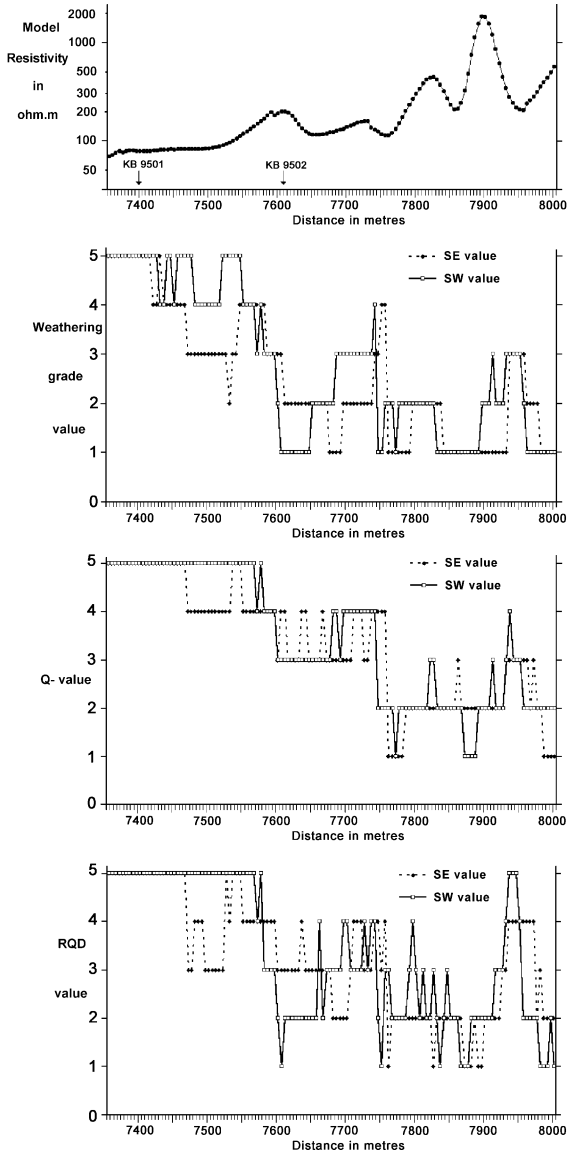

Fig. 11. Plot of the model resistivity, weathering grade, *Q* and RQD values along the tunnel route. Note that two separate measurements of the weathering grade, *Q* and RQD values were measured in the SE and SW tunnels.

Newton method agrees with the known geology from the boreholes despite the very large resistivity range. For a preliminary interpretation, particularly in the field during the course of a survey, this might be sufficiently accurate. The differences are in the secondary structures (such as the high resistivity structure below the 7830-m mark) that tend to be smoothed out by the quasi-Newton method. The model obtained with two recalculations of the Jacobian matrix is very similar to the Gauss–Newton model. Thus, recalculating the Jacobian matrix for the first two iterations might be a reasonable compromise between reducing the computer time and obtaining an accurate model even in situations with very large resistivity contrasts.

4. Conclusions

For models with small resistivity contrasts, there are no significant differences in the results obtained with the Gauss–Newton and quasi-Newton methods. For large resistivity contrasts, the Gauss–Newton method gives significantly more accurate results than the quasi-Newton method. However, even for such cases, the main features in the quasi-Newton model are similar to the Gauss–Newton model. In such cases, the quasi-Newton method is useful in giving a quick preliminary model of the subsurface, particularly during the course of a field survey. The combined method with one or two recalculations of the Jacobian matrix gives a satisfactory compromise between accuracy of the results and reduction in computer time. In the case of small data sets (with less than a few hundred data points) from 2D surveys, the time required for carrying out a full recalculation of the Jacobian matrix is small in relation to the time and cost of carrying out the survey, so the extra computer time needed might be worthwhile. However, in the case of large 2D and 3D data sets (which might have thousands of data points), the time required for a full recalculation of the Jacobian matrix can be a significant drawback. This can be especially pertinent if inversion tests with different models and different optimisation parameters are to be carried out. Similar tests have also been carried out in 3D inversion of resistivity data (Loke and Barker, 1996b; Loke and Dahlin, 1997). The results from the 3D tests are similar to those obtained in the above 2D tests.

In this paper, we have examined a combined method where the recalculation of the Jacobian matrix is carried out in the first few iterations only. Another possible scheme is to carry out the recalculation of the Jacobian matrix in the later part of the inversion process, for example, at fifth iteration, and then

proceeding with the inversion process for another one or two iterations using the quasi-Newton method (Oldenburg, personal communication). Preliminary tests indicate that calculating the Jacobian matrix at the first iteration and again at several iterations later might give better results for some data sets. Research is presently being carried out in the optimum method to distribute the recalculation of the Jacobian matrix in the inversion process.

Acknowledgements

The author, M.H.Loke, would like to acknowledge the support given by the School of Physics, Universiti Sains Malaysia. We would like to thank the Swedish National Rail Administration for permission to publish the Hallandsås data. We would also like to thank Prof. Oldenburg and an anonymous reviewer for their helpful comments that improved the final manuscript.

References

Barton, N., Lien, R., Lunde, J., 1974. Engineering classification of rock masses for the design of tunnel support. Rock Mechanics 6 (4), 189–236.

Broyden, C.G., 1965. A class of methods for solving nonlinear simultaneous equations. Mathematics of Computation 19, 577–593.

Burden, R.L., Faires, J.D., Reynolds, A.C., 1981. Numerical Analysis. Prindle, Webber & Schmidt, Boston, Mass.

Dahlin, T., 1996. 2D resistivity surveying for environmental and engineering applications. First Break 14, 275–283.

Dahlin, T., Sturk, R., 1998. Resistivity pre-investigations for the Hallandsås railway tunnel, Sweden. Procs. Underground '98, Stockholm, 7–9 June. Balkema, Rotterdam, pp. 135–141.

Dahlin, T., Bjelm, L., Svensson, C., 1996. Resistivity pre-investigation for the railway tunnel through Hallandsas, Sweden. Procs. 2nd EEGS European Section Meeting, Nantes, France, 109–113.

Dahlin, T., Bjelm, L., Svensson, C., 1999a. Use of electrical imaging in site investigations for a railway tunnel through the Hallandsås Horst, Sweden. Quarterly Journal of Engineering Geology 32 (2), 163–173.

Dahlin, T., Gass, R., Jeppsson, H., 1999b. Resistivity surveying as pre-investigation method for the Hallandsås tunnel project. Procs. 5th Meeting of the European Association for Environmental and Engineering Geophysics, 5–9 September 1999, Budapest, 2 pp.

Daniels, R.W., 1978. An Introduction to Numerical Methods and Optimization Techniques. Elsevier North-Holland, New York.

deGroot-Hedlin, C., Constable, S.C., 1990. Occam's inversion to generate smooth, two-dimensional models from magnetotelluric data. Geophysics 55, 1613–1624.

Dey, A., Morrison, H.F., 1979. Resistivity modelling for arbitrary shaped two-dimensional structures. Geophysical Prospecting 27, 1020–1036.

Edwards, L.S., 1977. A modified pseudosection for resistivity and induced-polarization. Geophysics 42, 1613–1624.

Goodman, R.E., 1993. Engineering Geology. Wiley, New York.

Griffiths, D.H., Barker, R.D., 1993. Two-dimensional resistivity imaging and modelling in areas of complex geology. Journal of Applied Geophysics 29, 211–226.

Loke, M.H., 2000. Topographic modelling in resistivity imaging inversion. 62nd EAGE Conference and Technical Exhibition Extended Abstracts, D-2.

Loke, M.H., Barker, R.D., 1996a. Rapid least-squares inversion of apparent resistivity pseudosections by a quasi-Newton method. Geophysical Prospecting 44, 131–152.

Loke, M.H., Barker, R.D., 1996b. Practical techniques for 3D resistivity surveys and data inversion. Geophysical Prospecting 44, 499–523.

Loke, M.H., Dahlin, T., 1997. A combined Gauss–Newton and quasi-Newton inversion method for the interpretation of apparent resistivity pseudosections. Procs. 3rd Meeting of the European Association for Environmental and Engineering Geophysics, 8–11 Sept. 1997, Aarhus, Denmark, 139–142.

McGillivray, P.R., Oldenburg, D.W., 1990. Methods for calculating Frechet derivatives and sensitivities for the non-linear inverse problem: a comparative study. Geophysical Prospecting 38, 499–524.

Niederleithinger, E., 1994. Use of high resolution geomagnetics, 2D-DC-geoelectrics and induced polarisation in environmental investigations. Paper presented at SAGEEP '94, Boston, USA.

Oldenburg, D.W., Li, Y., 1994. Inversion of induced polarization data. Geophysics 59, 1327–1341.

Press, W.H., Flannery, B.P., Teukolsky, S.A., Vetterling, W.T., 1988. Numerical Recipes in C. Cambridge Univ. Press, Cambridge, UK.

Rodi, W., Mackie, R.L., 2001. Nonlinear conjugate gradients algorithm for 2-D magnetotelluric inversion. Geophysics 66, 174–187.

Sasaki, Y., 1989. Two-dimensional joint inversion of magnetotelluric and dipole–dipole resistivity data. Geophysics 54, 254–262.

Sasaki, Y., Yoneda, Y., Matsuo, K., 1992. Resistivity imaging of controlled-source audiofrequency magnetotelluric data. Geophysics 57, 952–955.

Silvester, P.P., Ferrari, R.L., 1990. Finite Elements for Electrical Engineers, 2nd edn. Cambridge Univ. Press, Cambridge, UK.

Spiegel, R.J., Sturdivant, V.R., Owen, T.E., 1980. Modeling resistivity anomalies from localized voids under irregular terrain. Geophysics 45, 1164–1183.

Tong, L., Yang, C., 1990. Incorporation of topography into 2-D resistivity inversion. Geophysics 55, 354–361.